Reservoir-Free Decoherence in Flying Qubits

Nicolò Piccione,[1,2,3,*] Léa Bresque,[1,4] Andrew N. Jordan,[5,6,7] Robert S. Whitney,[8] and Alexia Auffèves[1,9,10]
[1]Université Grenoble Alpes, CNRS, Grenoble INP, Institut Néel, 38000 Grenoble, France
[2]Department of Physics, University of Trieste, Strada Costiera 11, 34151 Trieste, Italy
[3]Istituto Nazionale di Fisica Nucleare, Trieste Section, Via Valerio 2, 34127 Trieste, Italy
[4]The Abdus Salam International Center for Theoretical Physics (ICTP), Strada Costiera 11, 34151 Trieste, Italy
[5]Institute for Quantum Studies, Chapman University, Orange, California, 92866, USA
[6]Department of Physics and Astronomy, University of Rochester, Rochester, New York 14627, USA
[7]The Kennedy Chair in Physics, Chapman University, Orange, California 92866, USA
[8]Université Grenoble Alpes, CNRS, LPMMC, Grenoble 38000, France
[9]MajuLab, CNRS–UCA-SU-NUS-NTU International Joint Research Laboratory
[10]Centre for Quantum Technologies, National University of Singapore, 117543 Singapore, Singapore

(Received 16 May 2023; accepted 9 April 2024; published 30 May 2024)

An effective time-dependent Hamiltonian can be implemented by making a quantum system fly through an inhomogeneous potential, realizing, for example, a quantum gate on its internal degrees of freedom. However, flying systems have a spatial spread that will generically entangle the internal and spatial degrees of freedom, leading to decoherence in the internal state dynamics, even in the absence of any external reservoir. We provide formulas valid at all times for the dynamics, fidelity, and change of entropy for ballistic particles with small spatial spreads, quantified by Δx. This non-Markovian decoherence can be significant for ballistic flying qubits (scaling as Δx^2) but usually not for flying qubits carried by a moving potential well (scaling as Δx^6). We also discuss a method to completely counteract this decoherence for a ballistic qubit later measured.

DOI: 10.1103/PhysRevLett.132.220403

Flying qubits, such as flying Rydberg atoms [1–6], flying spin qubits [7–10], or flying electrons [10–17], have practical and fundamental significance. Practically, there is great hope to use the internal state of flying qubits to process and transport quantum information. This is a goal of recent experiments on flying electrons in solid state devices, with quantum information carried by the electron's spins [7–10], or its spatial distribution [10,11]. Similar ideas have long been applied to flying Rydberg atoms [1–5]. Fundamentally, they are the simplest examples of how time-dependent Hamiltonians emerge from time-independent ones, i.e., how nonautonomous dynamics emerge from autonomous ones [18]. This is used for measurement paradoxes [19–23], symmetries [24], quantum optics [25–28], quantum collision models [29–32], and quantum thermodynamics [6,29,31–34]. As a system flies through a spatially varying potential, its internal state experiences a time-dependent Hamiltonian. However, this is *only* true if the flying system is pointlike [31]. Otherwise, its internal degree of freedom (d.o.f.) also get entangled with its spatial d.o.f., causing decoherence of the internal d.o.f. This is a fundamental source of decoherence, intrinsic to the flying nature of the system. We remark that the internal d.o.f. does not have to be a qubit (i.e., a two-level system); it can have arbitrary structure, the qubit being the paradigmatic case.

In this Letter, we consider a quantum system that flies ballistically, i.e., at approximately constant velocity, with a small spatial spread, as drawn in Fig. 1. We analyze its internal dynamics for arbitrary internal structure. The wave packet's spatial spread causes noisy dynamics for the internal state, even in the absence of any external reservoirs. Thus, we refer to its effect as reservoir-free decoherence and we analytically characterize it. We quantify this in

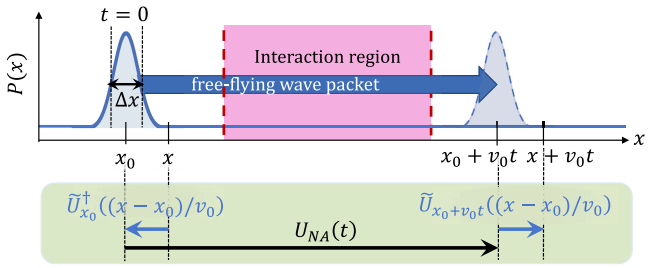

FIG. 1. A ballistic quantum system is moving at constant velocity to enter in and exit from an interaction region acting on its internal state. During the interaction the internal state associated with each position in the wave packet evolves differently due to the different time spent in the interaction region and free evolution region. The green box shows a decomposition of the internal state dynamics associated with the point x. This decomposition is the one we used to obtain our results; see text for details.

terms of the internal state's fidelity (compared to an ideal pointlike system), and its entropy change. Then, we apply our findings to flying qubits, and identify ways to reduce or completely nullify the reservoir-free decoherence. Finally, we estimate it for flying systems carried by a moving potential well, and find that it is much weaker than for ballistic flying systems.

Ballistic system's dynamics.—Consider a quantum system with arbitrary internal structure flying ballistically. We want its internal dynamics to correspond to a desired nonautonomous (i.e., time-dependent) dynamics given by the evolution operator $U_{\mathrm{NA}}(t)$, resulting from the time-dependent Hamiltonian $H_{\mathrm{NA}}(t)$. To do this, we let it fly through a one-dimensional potential so that the total, autonomous, Hamiltonian reads

$$H = \frac{\hat{p}^2}{2m} + H_0 + V(\hat{x}), \tag{1}$$

where m is the system's mass, $\hat{x}$ and $\hat{p}$ are its position and momentum operators, H_0 is the $\hat{x}$-independent part of the internal Hamiltonian and $V(\hat{x})$ the $\hat{x}$-dependent part.

In the ideal case of a particle with classical spatial d.o.f., we can assign to it a definite position $x_{\mathrm{cl}}(t)$ and momentum at any time. Then, the interaction term acts on the internal d.o.f. as $V(x_{\mathrm{cl}}(t))$. Assuming that the particle's momentum is constant, hence it moves at constant velocity v_0, its position is $x_{\mathrm{cl}}(t) = x_0 + v_0 t$, where x_0 is the particle's initial position. It follows that the internal state evolves as governed by the Hamiltonian $H_{\mathrm{NA}}(t) \equiv H_0 + V(x_0 + v_0 t)$. In the following, we consider what happens if the particle is not pointlike, i.e., is described by a wave packet of finite size initially centered at x_0. Then, $V(\hat{x})$ may also transfer energy between the particle's internal and spatial d.o.f., while entangling them.

Approximations.—Solving Eq. (1) can be involved, even for wave packets without internal d.o.f. hitting simple barriers [35,36]. The regime we are interested in is defined by two approximations. First, the kinetic energy changes induced by $V(\hat{x})$ are supposed to be negligible at all times with respect to the mean initial kinetic energy. Introducing p_0 the particle's initial average momentum and $\hat{q} = \hat{p} - p_0$, it yields $\langle \hat{q} \rangle \ll p_0$ and $\langle \hat{q}^2 \rangle \ll p_0^2$. This leads to the so-called quantum clock dynamics [19–21,37,38], which corresponds to linearizing the kinetic energy in solid-state physics (used for flying qubits in [11]). Equation (1) becomes

$$H \simeq v_0 \hat{q} + H_0 + V(\hat{x}), \tag{2}$$

where we drop the constant $p_0^2/(2m)$, with no effect on the dynamics, and the approximation involves dropping $\hat{q}^2/(2m)$. This means that the wave packet propagates without dispersion and at a constant group velocity (further simply dubbed velocity) $v_0 = p_0/m$.

Second, the particle should remain sufficiently localized at all times, such that its internal states typically accumulate a small phase difference over the entire wave packet. Introducing Δx the typical width of the wave packet and E_0 the typical energy scale of the internal Hamiltonian $H_0 + V(x)$, this condition means

$$\varepsilon \equiv \frac{\Delta x E_0}{\hbar v_0} \ll 1, \tag{3}$$

where the parameter ε plays a major role in our calculations, as we show below. For Gaussian wave packets, Heisenberg inequality is saturated ($\Delta x \Delta p = \hbar/2$), and $\varepsilon \ll 1$ can be written as $p_0 \Delta p/m \gg E_0$. It means that the spread of kinetic energy induced by the wave packet localization largely overcomes the internal energy scale: hence, the different spatial states resulting from the evolution of different internal states remain almost indistinguishable —in other words, the spatial d.o.f. carries a small amount of which path information on the internal d.o.f.

Starting from Eq. (2), the dynamics can be solved exactly, as shown in Sec. I of Supplemental Material (SM) [39]. We consider the particle to be completely outside of the interaction region at $t = 0$, as shown in Fig. 1. It then makes sense to consider spatial and internal d.o.f. to be initially uncorrelated. The internal state at time t is given by

$$\rho_I(t) = \int_{-\infty}^{+\infty} A_0(x,x) \tilde{U}_x(t) \rho_0 \tilde{U}_x^\dagger(t) \mathrm{d}x, \tag{4}$$

with $A_0(x,x)$ the initial probability density of finding the particle at point x, ρ_0 the initial internal state, and

$$\tilde{U}_x(t) = \mathcal{T} \exp\left[-\frac{i}{\hbar} \int_0^t \mathrm{d}s \, H_{\mathrm{NA}}\left(s + \frac{x - x_0}{v_0} \right) \right], \tag{5}$$

where $\mathcal{T}$ is the time-ordering operator. $\tilde{U}_x(t)$ is the evolution operator for the internal state associated with position x in the wave packet. Hence, different parts of the wave packet (i.e., different x) have different dynamics, even though each part of the wave packet goes through the same potential $V(\hat{x})$ during its flight. This is the origin of the entanglement between the spatial and internal d.o.f., leading to the reservoir-free decoherence.

For a time t_f such that the wave packet has completely gone through the potential region, the reservoir-free decoherence can be intuitively explained as follows. For each initial position x of the particle within the wave packet, the internal state evolves according to the ideal dynamics one would have starting from x instead of x_0. This dynamics splits into three parts: before, during, and after the interaction region. The interaction region acts in the same way for each starting position x, but the respective durations of the free evolution steps depend on x. If the

dynamics in the interaction region does not commute with the free one, then each x gives rise to a different total evolution, hence entangling the spatial and internal d.o.f. Otherwise, the evolution is the same for each starting point and there is no reservoir-free decoherence. This can happen, for example, if $[V(\hat{x}), H_0] = 0$ or if $H_{\rm NA}(t)$ changes adiabatically.

Approximate dynamics.—We now solve the internal d.o.f. dynamics in the regime of localized wave packet defined by $\varepsilon \ll 1$. Let the flying particle's initial wave packet be localized in space, centered at x_0 with a spread $\Delta x = [\langle \hat{x}^2 \rangle - \langle \hat{x} \rangle^2]^{1/2}$, see Fig. 1. The wave packet moves from left to right at constant velocity v_0, so it is centered at $x_0 + v_0 t$ at time t. The part of the wave function initially at x_0 has internal evolution $U_{\rm NA}(t) \equiv \tilde{U}_{x_0}(t)$. For other initial x, we can decompose their evolution as shown in the green box of Fig. 1; evolving from x to x_0 using $\tilde{U}^\dagger_{x_0}((x - x_0)/v_0)$, from x_0 to $x_0 + v_0 t$ using $U_{\rm NA}(t)$, and from $x_0 + v_0 t$ to $x + v_0 t$ using $\tilde{U}_{x_0+v_0 t}((x - x_0)/v_0)$. Then, assuming $\varepsilon \ll 1$, we can expand $\tilde{U}^\dagger_{x_0}((x - x_0)/v_0)$ and $\tilde{U}_{x_0+v_0 t}((x - x_0)/v_0)$ by means of Taylor expansions (see Secs. II and III of SM [39]). This gives simple expressions for the dynamics and quantities of interest, in the regime in which the internal state ideal dynamics is only weakly perturbed by the spatial spread of the wave packet.

In this regime, the internal state's reduced density matrix at time t, after tracing over the spatial wave function (see Sec. III of SM [39]), is

$$\rho_I(t) \simeq \rho_{\rm NA}(t) + \varepsilon^2 \mathcal{C}(t), \tag{6}$$

where $\rho_{\rm NA}(t) = U_{\rm NA}(t)\rho_0 U^\dagger_{\rm NA}(t)$ is the nonautonomous ideal dynamics (that of the wave packet's center), and

$$\mathcal{C}(t) = \{[H_{\rm NA}, U[H_0, \rho_0]U^\dagger] - \frac{i\hbar}{2}[\partial_t H_{\rm NA}, U\rho_0 U^\dagger] + U D_{H_0}(\rho_0)U^\dagger + D_{H_{\rm NA}}(U\rho_0 U^\dagger)\}/E_0^2, \tag{7}$$

is the correction term, with $D_X(\rho) = X\rho X^\dagger - (1/2)\{X^\dagger X, \rho\}$, and U (respectively $H_{\rm NA}$) being shorthand for $U_{\rm NA}(t)$ [respectively, $H_{\rm NA}(t)$]. Importantly, Eqs. (6) and (7) reveal that the deviation from ideal dynamics scales as Δx^2 but its form [encoded in $\mathcal{C}(t)$] is independent of Δx. Moreover, at a practical level, Eqs. (6) and (7) are easy to solve: unlike Eq. (1), they do not involve the large Hilbert space of the spatial d.o.f., and standard perturbation theory can be applied to find $U_{\rm NA}(t)$ (see, e.g., Ref. [43]). Below we exploit these analytic expressions to quantify the impact of the reservoir-free decoherence.

Fidelity and entropy.—We consider two ways of characterizing how close the internal dynamics are to ideal [44,45]: (i) the fidelity between real and ideal internal state, and (ii) the von Neumann entropy change of the real internal state. In Sec. IV of SM [39], we derive both from Eqs. (6) and (7), using a method from Ref. [46]. When the initial internal state is pure, we define the ideal evolution as $|\psi_{\rm NA}(t)\rangle\langle\psi_{\rm NA}(t)|$. Then, the fidelity $F(t) \equiv \langle\psi_{\rm NA}(t)|\rho_I(t)|\psi_{\rm NA}(t)\rangle$, and the von Neumann entropy $S(t) \equiv -{\rm Tr}\{\rho_I(t)\ln\rho_I(t)\}$ are

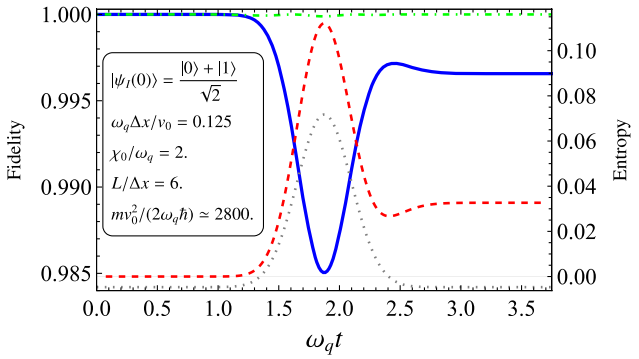

FIG. 2. A qubit flying through an inhomogeneous potential. The qubit bare Hamiltonian is $H_0 = (1/2)\hbar\omega_q\sigma_z$ while the interaction term is $V(\hat{x}) = \frac{1}{2}\hbar\chi_0\sigma_x \exp[-\pi x^2/L^2]$, sketched as the dotted gray curve. Since $H_{\rm NA}$ does not commute with itself at different times even the ideal dynamics are nontrivial, so we obtain both $\rho_{\rm NA}$ and ρ_I numerically by adapting a method from Ref. [48]. The initial state is a Gaussian wave packet with spatial spread Δx centered at x_0 and mean wave vector k_0, with internal state $(|0\rangle + |1\rangle)/\sqrt{2}$. The continuous blue line represents the fidelity in Eq. (8) as the qubit flies. The dot-dashed green line is the fidelity of the approximate state Eq. (6) relative to an exact evolution of Eq. (1); it is close to one, showing that the approximation is very good. Finally, the red dashed line represents the internal state's von Neumann entropy (in bits) in Eq. (9).

$$F(t) \simeq 1 - \varepsilon^2 \left|\langle\psi_{\rm NA}(t)|\mathcal{C}(t)|\psi_{\rm NA}(t)\rangle\right|, \tag{8}$$

$$S(t) \simeq \varepsilon^2 {\rm Tr}\{\mathcal{C}_\perp(t) - \mathcal{C}_\perp(t)\ln[\varepsilon^2\mathcal{C}_\perp(t)]\}, \tag{9}$$

where $\mathcal{C}_\perp(t) = (1 - |\psi_{\rm NA}(t)\rangle\langle\psi_{\rm NA}(t)|)\mathcal{C}(t)(1 - |\psi_{\rm NA}(t)\rangle\times\langle\psi_{\rm NA}(t)|)$ is the part of $\mathcal{C}(t)$ orthogonal to $|\psi_{\rm NA}(t)\rangle$. The case of a mixed initial internal state is discussed in Sec. IV of SM [39]. Equations (6)–(9) are the main results of this Letter.

Equations (6)–(9) are valid at all times during the dynamics, giving, for example, a qubit's fidelity and entropy as its wave packet flies through the interaction region, as is done in Fig. 2, which shows that $F(t)$ and $S(t)$ are both nonmonotonic functions of time. Equation (4) implies that if $\rho_0 \propto \mathbb{I}$ then $\rho_I(t) \propto \mathbb{I}$ at any time t, i.e., the dynamics is unital. This implies that the reservoir-free decoherence is non-Markovian [47]. A short but rigorous proof of this statement is given in Sec. IV of SM [39].

Notice that, in general, $F(t) < 1$ and $S(t) > 0$ while the particle is inside the interaction region even if the gate is perfectly implemented, such as the PHASE and CPHASE gates discussed below.

Example with ballistic qubits.—Let $H_0 = \frac{1}{2}\hbar\omega_q\sigma_z$, where σ_z is the usual Pauli operator, and ω_q is the qubit frequency. We consider that the wave packet entirely passes through an interaction region whose ideal dynamics perform a desired gate operation at final time t_f, where we recall that $H_{\rm NA}(t_f) = H_0$ and the typical energy scale is $E_0 = \hbar\omega_q$. We then evaluate the effect of the reservoir-free decoherence caused by the wave packet's spatial spread. Notice that there is an infinite number of possible potentials $V(\hat{x})$ which would ideally implement a specific gate at final time. However, neither the final correction term, nor the final fidelity and entropy depend on this specific choice.

As the first example, let us consider a NOT gate, with ideal dynamics given by $U_{\rm NA}(t_f) = -i\sigma_x$, acting on an initial state $\rho_0 = |\psi_I(0)\rangle\langle\psi_I(0)|$, with $|\psi_I(0)\rangle = \sqrt{a_0}|0\rangle + e^{i\theta}\sqrt{a_1}|1\rangle$, in the eigenbasis of H_0. Then, $\mathcal{C}(t_f) = -2[e^{i\theta}\sqrt{a_0 a_1}|0\rangle\langle 1| + \text{H.c.}]$, and

$$F(t_f) = 1 - K(t_f), \qquad S(t_f) = K(t_f)\{1 - \ln[K(t_f)]\}, \quad (10)$$

where $K(t_f) \equiv 4a_0a_1(\omega_q\Delta x/v_0)^2$. As expected, the wave packet's spatial spread reduces the gate fidelity, while increasing the qubit's entropy, for any initial state except eigenstates of H_0.

As second example, let us consider a PHASE gate, whose ideal dynamics are $U_{\rm NA}(t_f) = \exp[-i(\phi/2)\sigma_z]$. Then $[U_{\rm NA}(t_f), H_0] = 0$, which implies $F(t_f) = 1$ and $S(t_f) = 0$ for all choices of ρ_0. Although entanglement is built during the interaction, the internal state associated with each position in the wave packet undergoes the same dynamics once the wave packet has completely passed through the interaction region. In other words, $\tilde{U}_x(t_f) = U_{\rm NA}(t_f)$, $\forall\ x$ [cf. Eq. (5)].

More generally, an arbitrary gate operation has fidelity and entropy of the form given in Eq. (10), but the quantity K will be given by $(\omega_q\Delta x/v_0)^2$ multiplied by a prefactor which will depend on the gate operation (given by $U_{\rm NA}$) as well as the initial state ρ_0.

Two-qubit gate example.—Our Eqs. (1)–(9) can also describe the dynamics of two flying systems when their interaction only depends on their distance and we neglect the center of mass dynamics; see also Sec. V of SM [39]. Therefore, we can consider two flying qubits (1 and 2) traveling at different velocities along parallel 1D tracks. As one qubit flies past the other, their interaction $V(|\hat{x}_1 - \hat{x}_2|)$ performs a desired gate operation between them. A CPHASE gate is unaffected by the reservoir-free decoherence, because the proper evolution of each qubit (under H_1 and H_2) commutes with the gate operation, so $\mathcal{C}(t_f) = 0$. However, the CNOT gate is affected by noise scaling as $p(\Delta x_1^2 + \Delta x_2^2)/[\hbar^2(v_1 - v_2)^2]$ (see Sec. V of SM [39]) where p is the population of the control qubit and we assumed the two qubit spatial states to be initially uncorrelated. The $\mathcal{C}(t_f)$ term has the same form as for the NOT gate [see above Eq. (10)] when the control qubit is in state $\langle 1|$ and is zero otherwise. The fidelity is then given by $F = 1 - pK$ where K is defined as before but now refers to the qubit on which the NOT part of the gate acts. The entropy is easily computed, but its formula is more involved and not given here.

Experimental consequences.—Ballistic electrons can be injected into quantum Hall edge states on demand (Levitons, etc.), and made to interact [49–52]. They typically have $\Delta x/v_0 \sim 10^{-10}$ s [50,51]. If the electron's spin were used as a qubit, one would have $\omega_q \sim 10^{-10}\,\text{s}^{-1}$, since the B fields $\gtrsim 1$ T. Then, the reservoir-free decoherence would be strong, $\omega_q\Delta x/v_0 \sim 1$, giving fidelities much too small for quantum gate operations.

Achieving higher fidelities would require lower magnetic fields to get smaller ω_q. This might be experimentally realizable with electrons flying ballistically in a waveguide similar to [11] with B fields of mT, allowing $\omega_q \sim 10^{-13}\,\text{s}^{-1}$. If the injection into this waveguide could be done with a similar Δx as the injection into an edgestate, extremely high fidelities could be attained, with $1 - F \sim (\omega_q\Delta x/v_0)^2 \sim 10^{-6}$.

Avoiding reservoir-free decoherence.—The reservoir-free decoherence depends on the fact that, for each spatial point in the traveling wave function, the internal state experiences a different dynamics. However, if the initial internal state is an eigenstate of the bare Hamiltonian, H_0 (such as the ground state) it does not evolve prior to entering the interaction region and, once out of it, its evolution does not change the populations of states in the eigenbasis of H_0. Thus, the final internal state may be decohered in this energy eigenbasis, but the eigenstate's populations are the same as for the ideal dynamics.

This implies that reservoir-free decoherence plays no role whenever the system starts in an eigenstate of H_0, and it flies through potentials that (i) rotate the internal state to the desired superposition, (ii) perform a series of gate operations, and (iii) prepare the final state for an energy eigenbasis measurement [53]. This is the case in experiments on flying Rydberg atoms [6], or flying electrons in waveguides [11], explaining their negligible decoherence despite their wave packets' large spatial spreads.

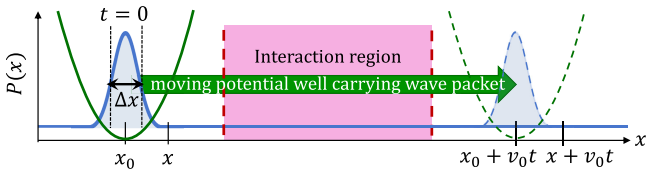

FIG. 3. A flying quantum system that is trapped in a potential well that moves at constant velocity, carrying the quantum system through the interaction region.

Qubits carried by a moving potential.—Finally, we consider qubits that fly by being trapped in a moving harmonic potential well [54], as in Fig. (3), sometimes called flying qubits and sometimes called surfing or shuttling qubits [7–10]. Section IV of SM [39] shows that the quantization of the wave function in the moving harmonic potential vastly reduces the reservoir-free decoherence compared to the ballistic qubits that are the principle subject of this Letter. Intuitively, this can be understood semiclassically: the particle undergoes a harmonic motion around the center of the moving trap, effectively averaging out the differences in internal dynamics in different parts of the wave packet. Therefore, all parts of the wave packet have internal dynamics closer to the wave packet's center than in the ballistic case. As a result, the order δx^2 term in Eq. (6) is replaced by a term which we estimate to be smaller than $36(m^2/\hbar^2 v_0^2 \tau^4)\Delta x^6$, where τ is the time needed to apply the desired gate [55]. This term is of order 10^{-8} or smaller in most experiments (see Sec. VI-C of SM [39]), which is small enough to completely neglect. Hence, reservoir-free decoherence can be effectively removed by switching from ballistic qubits to qubits carried by a moving harmonic potential wells.

Conclusions.—We considered flying quantum systems as bipartite systems divided into spatial and internal d.o.f., focusing on the case of ballistic particles with a narrow spatial distribution. We analytically investigated the effects of the wave packet's spatial spread on the internal state dynamics, which experiences reservoir-free decoherence (decoherence without an external reservoir) due to the entanglement between spatial and internal d.o.f. We derived the internal state full dynamics, which is necessary in quantum thermodynamics, if one wants to go beyond our calculations of entropy, and quantify generalized work and heat using definitions like in Refs. [56,57]. Finally, we estimated this effect to be practically negligible for surfing or shuttling qubits. In the future, it would be interesting to explore how tuning the shape of the potential can reduce even more the reservoir-free decoherence, which fundamentally affects every flying quantum system.

This work was supported by the John Templeton Foundation (Grant No. 61835). N. P. acknowledges the support by PNRR NQSTI Spoke 1 "Foundations and architectures for quantum information processing and communication" CUP: J93C22001510006. L. B. acknowledges the support by PNRR MUR project PE0000023-NQSTI. R. W. acknowledges the ANR Project "TQT" (ANR-20-CE30-0028). A. A. acknowledges the National Research Foundation, Singapore and A*STAR under its CQT Bridging Grant, the Plan France 2030 through the projects NISQ2LSQ ANR-22-PETQ-0006 and OQuLus ANR-23-PETQ-0013, ANR Research Collaborative Project "Qu-DICE" (Grant No. ANR-PRC-CES47) and the Foundational Questions Institute Fund (Grants No. FQXi-IAF19-01 and No. FQXi-IAF19-05). A. A. and R. W. acknowledge the ANR Research Collaborative Project "QuRes" (Grant No. ANR-PRC-CES47-0019).

*nicolo'.piccione@units.it

[1] S. Haroche and J.-M. Raimond, *Exploring The Quantum: Atoms, Cavities, and Photons* (Oxford University Press, New York, 2006).
[2] S. Haroche, M. Brune, and J. M. Raimond, From cavity to circuit quantum electrodynamics, Nat. Phys. **16**, 243 (2020).
[3] S. Osnaghi, P. Bertet, A. Auffeves, P. Maioli, M. Brune, J. M. Raimond, and S. Haroche, Coherent control of an atomic collision in a cavity, Phys. Rev. Lett. **87**, 037902 (2001).
[4] A. Rauschenbeutel, G. Nogues, S. Osnaghi, P. Bertet, M. Brune, J. M. Raimond, and S. Haroche, Coherent operation of a tunable quantum phase gate in cavity QED, Phys. Rev. Lett. **83**, 5166 (1999).
[5] A. Rauschenbeutel, G. Nogues, S. Osnaghi, P. Bertet, M. Brune, J.-M. Raimond, and S. Haroche, Step-by-step engineered multiparticle entanglement, Science **288**, 2024 (2000).
[6] B.-L. Najera-Santos, P. A. Camati, V. Métillon, M. Brune, J.-M. Raimond, A. Auffèves, and I. Dotsenko, Autonomous Maxwell's demon in a cavity QED system, Phys. Rev. Res. **2**, 032025(R) (2020).
[7] B. Jadot, P.-A. Mortemousque, E. Chanrion, V. Thiney, A. Ludwig, A. D. Wieck, M. Urdampilleta, C. Bäuerle, and T. Meunier, Distant spin entanglement via fast and coherent electron shuttling, Nat. Nanotechnol. **16**, 570 (2021).
[8] A. Noiri, K. Takeda, T. Nakajima, T. Kobayashi, A. Sammak, G. Scappucci, and S. Tarucha, A shuttling-based two-qubit logic gate for linking distant silicon quantum processors, Nat. Commun. **13**, 5740 (2022).
[9] I. Seidler, T. Struck, R. Xue, N. Focke, S. Trellenkamp, H. Bluhm, and L. R. Schreiber, Conveyor-mode single-electron shuttling in Si/SiGe for a scalable quantum computing architecture, npj Quantum Inf. **8**, 1 (2022).
[10] H. Edlbauer, J. Wang, T. Crozes, P. Perrier, S. Ouacel, C. Geffroy, G. Georgiou, E. Chatzikyriakou, A. Lacerda-Santos, X. Waintal *et al.*, Semiconductor-based electron flying qubits: Review on recent progress accelerated by numerical modelling, Eur. Phys. J. Quantum Technol. **9**, 21 (2022).
[11] M. Yamamoto, S. Takada, C. Bäuerle, K. Watanabe, A. D. Wieck, and S. Tarucha, Electrical control of a solid-state flying qubit, Nat. Nanotechnol. **7**, 247 (2012).
[12] C. Bäuerle, D. C. Glattli, T. Meunier, F. Portier, P. Roche, P. Roulleau, S. Takada, and X. Waintal, Coherent control of single electrons: A review of current progress, Rep. Prog. Phys. **81**, 056503 (2018).
[13] S. Takada, H. Edlbauer, H. V. Lepage, J. Wang, P.-A. Mortemousque, G. Georgiou, C. H. Barnes, C. J. Ford, M. Yuan, P. V. Santos *et al.*, Sound-driven single-electron transfer in a circuit of coupled quantum rails, Nat. Commun. **10**, 4557 (2019).

[14] L. Freise, T. Gerster, D. Reifert, T. Weimann, K. Pierz, F. Hohls, and N. Ubbelohde, Trapping and counting ballistic nonequilibrium electrons, Phys. Rev. Lett. **124**, 127701 (2020).
[15] H. Edlbauer, J. Wang, S. Ota, A. Richard, B. Jadot, P.-A. Mortemousque, Y. Okazaki, S. Nakamura, T. Kodera, N.-H. Kaneko *et al.*, In-flight distribution of an electron within a surface acoustic wave, Appl. Phys. Lett. **119**, 114004 (2021).
[16] J. Wang, H. Edlbauer, A. Richard, S. Ota, W. Park, J. Shim, A. Ludwig, A. D. Wieck, H.-S. Sim, M. Urdampilleta, T. Meunier, T. Kodera, N.-H. Kaneko, H. Sellier, X. Waintal, S. Takada, and C. Bäuerle, Coulomb-mediated antibunching of an electron pair surfing on sound, Nat. Nanotechnol. **18**, 721 (2023).
[17] C. Henkel and R. Folman, Internal decoherence in nano-object interferometry due to phonons, AVS Quantum Sci. **4**, 025602 (2022).
[18] In fields such as quantum thermodynamics, a system is described as autonomous if the Hamiltonian describing it is time independent.
[19] Y. Aharonov and T. Kaufherr, Quantum frames of reference, Phys. Rev. D **30**, 368 (1984).
[20] Y. Aharonov, J. Oppenheim, S. Popescu, B. Reznik, and W. G. Unruh, Measurement of time of arrival in quantum mechanics, Phys. Rev. A **57**, 4130 (1998).
[21] N. Gisin and E. Zambrini Cruzeiro, Quantum measurements, energy conservation and quantum clocks, Ann. Phys. (Berlin) **530**, 1700388 (2018).
[22] S. Rogers and A. N. Jordan, Postselection and quantum energetics, Phys. Rev. A **106**, 052214 (2022).
[23] A. N. Jordan and I. A. Siddiqi, *Quantum Measurement: Theory and Practice* (Cambridge University Press, Cambridge, England, 2024).
[24] R. S. Whitney, A. Shnirman, and Y. Gefen, Towards a dephasing diode: Asymmetric and geometric dephasing, Phys. Rev. Lett. **100**, 126806 (2008).
[25] B.-G. Englert, J. Schwinger, A. Barut, and M. Scully, Reflecting slow atoms from a micromaser field, Europhys. Lett. **14**, 25 (1991).
[26] M. O. Scully, G. M. Meyer, and H. Walther, Induced emission due to the quantized motion of ultracold atoms passing through a micromaser cavity, Phys. Rev. Lett. **76**, 4144 (1996).
[27] J. Larson and M. Abdel-Aty, Cavity QED nondemolition measurement scheme using quantized atomic motion, Phys. Rev. A **80**, 053609 (2009).
[28] A. Mercurio, S. De Liberato, F. Nori, S. Savasta, and R. Stassi, Flying atom back-reaction and mechanically generated photons from vacuum, arXiv:2209.10419.
[29] S. L. Jacob, M. Esposito, J. M. R. Parrondo, and F. Barra, Thermalization induced by quantum scattering, PRX Quantum **2**, 020312 (2021).
[30] F. Ciccarello, S. Lorenzo, V. Giovannetti, and G. M. Palma, Quantum collision models: Open system dynamics from repeated interactions, Phys. Rep. **954**, 1 (2022).
[31] S. L. Jacob, M. Esposito, J. M. R. Parrondo, and F. Barra, Quantum scattering as a work source, Quantum **6**, 750 (2022).
[32] J. Tabanera, I. Luque, S. L. Jacob, M. Esposito, F. Barra, and J. M. R. Parrondo, Quantum collisional thermostats, New J. Phys. **24**, 023018 (2022).
[33] F. Binder, L. Correa, C. Gogolin, J. Anders, and G. Adesso, *Thermodynamics in the Quantum Regime* (Springer International Publishing, New York, 2018).
[34] G. D. Chiara, G. Landi, A. Hewgill, B. Reid, A. Ferraro, A. J. Roncaglia, and M. Antezza, Reconciliation of quantum local master equations with thermodynamics, New J. Phys. **20**, 113024 (2018).
[35] V. Los and N. Los, Exact solution of the one-dimensional time-dependent Schrödinger equation with a rectangular well/barrier potential and its applications, Theor. Math. Phys. **177**, 1706 (2013).
[36] N. Riahi, Solving the time-dependent Schrödinger equation via laplace transform, Quantum Stud. Math. Found. **4**, 103 (2017).
[37] A. S. Malabarba, A. J. Short, and P. Kammerlander, Clock-driven quantum thermal engines, New J. Phys. **17**, 045027 (2015).
[38] S. Sołtan, M. Frączak, W. Belzig, and A. Bednorz, Conservation laws in quantum noninvasive measurements, Phys. Rev. Res. **3**, 013247 (2021).
[39] See Supplemental Material at http://link.aps.org/supplemental/10.1103/PhysRevLett.132.220403, which includes Refs. [40–42] for detailed calculations and proofs of the results reported in the main text.
[40] C. Xiao-Yu, Perturbation theory of von Neumann entropy, Chin. Phys. B **19**, 040308 (2010).
[41] C. Cohen-Tannoudji, B. Diu, and F. Laloë, *Quantum Mechanics, Volume 1: Basic Concepts, Tools, and Applications* (John Wiley & Sons, New York, 2019).
[42] B. C. Hall, *Quantum Theory for Mathematicians* (Springer, New York, 2013), Vol. 267.
[43] L. Bresque, Énergétique de la mesure quantique, Ph.D. thesis, Université Grenoble Alpes, 2022.
[44] H.-P. Breuer and F. Petruccione, *The Theory of Open Quantum Systems* (Oxford University Press, New York, 2007).
[45] M. A. Nielsen and I. L. Chuang, *Quantum Computation and Quantum Information: 10th Anniversary Edition* (Cambridge University Press, Cambridge, England, 2010).
[46] M. R. Grace and S. Guha, Perturbation theory for quantum information, *Proceedings of the 2022 IEEE Information Theory Workshop (ITW), Mumbai, India* (IEEE, New York, 2022), pp. 500–505, 10.1109/ITW54588.2022.9965836.
[47] S. Das, S. Khatri, G. Siopsis, and M. M. Wilde, Fundamental limits on quantum dynamics based on entropy change, J. Math. Phys. (N.Y.) **59**, 012205 (2018).
[48] R. Schmied, *Using Mathematica for Quantum Mechanics* (Springer, Singapore, 2020).
[49] J. Dubois, T. Jullien, F. Portier, P. Roche, A. Cavanna, Y. Jin, W. Wegscheider, P. Roulleau, and D. C. Glattli, Minimal-excitation states for electron quantum optics using levitons, Nature (London) **502**, 659 (2013).
[50] V. Freulon, A. Marguerite, J.-M. Berroir, B. Plaçais, A. Cavanna, Y. Jin, and G. Fève, Hong-Ou-Mandel experiment for temporal investigation of single-electron fractionalization, Nat. Commun. **6**, 6854 (2015).

[51] M. Kataoka, N. Johnson, C. Emary, P. See, J. P. Griffiths, G. A. C. Jones, I. Farrer, D. A. Ritchie, M. Pepper, and T. J. B. M. Janssen, Time-of-flight measurements of single-electron wave packets in quantum Hall edge states, Phys. Rev. Lett. **116**, 126803 (2016).

[52] D. Ferraro, F. Ronetti, L. Vannucci, M. Acciai, J. Rech, T. Jockheere, T. Martin, and M. Sassetti, Hong-Ou-Mandel characterization of multiply charged Levitons, Eur. Phys. J. Spec. Top. **227**, 1345 (2018).

[53] Any internal-state observable can be measured by performing a unitary rotation followed by a measurement of populations in the energy eigenbasis of H_0.

[54] Here, we are interested in a regime where the nonautonomous dynamics is well-but-not-perfectly implemented, just as we were for ballistic qubits earlier. As such, the choice of harmonic trap potential is of general interest, as many potentials behave harmonically around their minima for well-trapped particles.

[55] This Δx^6 scaling assumes a harmonic trapping potential. While different Δx scaling occurs for less usual shapes of trapping potentials, our SM [39] shows it to be Δx^6 for any potential characterized by a single length scale Δx. It shows that an infinite square well also has Δx^6 scaling, but with a prefactor that is 3 orders of magnitude larger than for the harmonic potential.

[56] H. Weimer, M. J. Henrich, F. Rempp, H. Schröder, and G. Mahler, Local effective dynamics of quantum systems: A generalized approach to work and heat, Europhys. Lett. **83**, 30008 (2008).

[57] H. Hossein-Nejad, E. J. O'Reilly, and A. Olaya-Castro, Work, heat and entropy production in bipartite quantum systems, New J. Phys. **17**, 075014 (2015).